BOR Papers in Press. Published on November 9, 2016 as DOI:10.1095/biolreprod.116.142711

MicroRNAs are stored in the human MII oocyte and their expression profile changes in reproductive aging[1]

Running Title: MicroRNAs and human oocytes

Rosalia Battaglia,[3] Maria Elena Vento,[4] Marco Ragusa,[3] Davide Barbagallo,[3] Alessandro La Ferlita,[3] Giovanna Di Emidio,[5] Placido Borzì,[4] Paolo Giovanni Artini,[6] Paolo Scollo,[4] Carla Tatone,[5] Michele Purrello,[3] and Cinzia Di Pietro[2,3]
[3]Department of Biomedical and Biotechnological Science, Section of Biology and Genetics, *Giovanni Sichel*, University of Catania, Catania, Italy
[4]IVF Unit, Cannizzaro Hospital, Catania, Italy
[5]Department of Life, Health and Environmental Sciences, University of L'Aquila, L'Aquila, Italy
[6]Department of Experimental and Clinical Medicine, Division of Gynecology and Obstetrics, University of Pisa, Pisa, Italy

[1]This work was partially supported by a grant from Bio-nanotech Research and Innovation Tower, BRIT PONa3_00136, University of Catania.
[2]Correspondence: Cinzia Di Pietro, Department of Biomedical and Biotechnological Science, Section of Biology and Genetics, *Giovanni Sichel*, University of Catania, Via S Sofia 87, 95030 Catania, Italy. E-mail: dipietro@unict.it

ABSTRACT
Maternal RNAs are synthesized by the oocyte during its growth, some of them are utilized for oocyte-specific processes and metabolism, others are stored and used during early development before embryonic genome activation. The appropriate expression of complex sets of genes is needed for oocyte maturation and early embryo development. In spite of the basic role of non-coding RNAs in the regulation of gene expression, few studies have analyzed their role in human oocytes. In this study, we identified the microRNAs expressed in human MII oocytes and found that some of them are able to control pluripotency, chromatin remodeling and early embryo development. We demonstrated that 12 microRNAs are differentially expressed in women of advanced reproductive age and by bioinformatics analysis we identified their mRNA targets, expressed in human oocytes and involved in the regulation of pathways altered in reproductive aging. Finally, we found the upregulation of miR-29a-3p, miR-203a-3p and miR-494-3p, evolutionary conserved microRNAs, also in aged mouse oocytes and demonstrated that their overexpression is antithetically correlated with the downregulation of Dnmt3a, Dnmt3b, Pten and Tfam. We propose that oocyte microRNAs perform an important regulatory function in human female germ cells and their altered regulation could explain the changes occurring in oocyte aging.

Summary Sentence: Expression profiles of human oocyte microRNAs change in women of advanced reproductive age; differentially expressed miRNAs target genes involved in reproductive aging.

Key words: MicroRNAs, Human oocyte, Stemness, Reproductive Aging

INTRODUCTION

The latest data published by ENCODE (Encyclopedia of DNA Elements) Project Consortium reported that at least 75% of the human nuclear genome is transcribed, and most of the transcriptome is comprised of RNAs (non-coding RNAs) that are not translated into proteins [1-3]. Some of them may be considered *constitutive*, as they are abundantly and ubiquitously expressed and provide essential functions to the cells (rRNA, tRNA, snRNA) [3]. Others may be considered *regulatory* ncRNAs, since they are involved in different steps of gene expression. Regulatory ncRNAs are classified according their size as small ncRNAs (≤ 200 nt) or long ncRNAs (> 200 nt). Small ncRNAs, including microRNAs (miRNAs), small interfering RNAs (siRNAs) and PIWI element-interacting RNAs (piRNAs), are involved in gene regulation as post-transcriptional regulators or as elements of chromatin-modifying complexes [3]. MiRNAs are by far the most characterized both structurally and functionally. They regulate gene expression by binding to mRNA target sites in the 3' untranslated region (UTR) with partial or full complementarity: in the first case, miRNAs reduce translation and stability of their targets, in the second they cause target degradation [4]. Their central biomolecular role has been amply demonstrated and the same holds true for their involvement in human diseases: variations of their sequence, expression, and ensuing biomolecular functions have been detected in different pathologies, particularly in cancer [5, 6]. In reproductive biology, different studies have investigated the function of miRNAs in ovarian development, in oocyte differentiation, in follicular maturation, and their role in ovarian disease has been documented [7]. Oocyte differentiation occurs through protracted and complex processes beginning during embryonic life and ends at the moment that the MII oocyte is ovulated. The correct sequence of events, occurring during this extended period of time, as well as the constant dialogue between the germ cell and somatic cells within the ovarian follicle, establish the oocyte quality and pregnancy outcome. In fact, the production of a fully competent oocyte, ready for fertilization, represents one of the most important factors contributing to reproductive success [8].

Understanding the complex pathways regulating oocyte growth and maturation is important not only in basic research, but represents the first step in prognosis, diagnosis and therapy in reproductive medicine and could improve pregnancy success in ART. Regulation of gene expression represents one of the most important cellular processes determining oocyte quality. In fact, during growth the oocytes accumulate RNAs (maternal RNAs) that will be used for meiosis resumption or during the first phases of development before genomic activation of the embryo [9]. Several studies have focused on mRNAs, demonstrating the importance of the oocyte transcriptome in determining oocyte quality, but to date, very few studies are available on miRNA expression profiles in human female germ cells and on their biological function. [9]. MiRNAs have been identified in oocytes from numerous organisms, from zebrafish to humans, but today their biological role remains relatively unknown, especially in humans [10-16]. Moreover, the data obtained on murine models are controversial. Mouse germ cells produce small ncRNAs, in fact, cloning and sequencing of RNAs from murine oocytes revealed three classes of small ncRNAs: miRNAs, piRNAs, and endo-siRNAs [17, 18]. In 2007, it was suggested that mouse maternal miRNAs are essential for oocyte maturation and early embryo development [19, 20]. By preventing production of miRNAs, throughout deletion of Dicer (dsRNA processing enzyme), which catalyses the final cytoplasmic cleavage and generates mature miRNAs, the authors observed aberrant spindles, meiosis arrest and inhibition of zygote development [19, 20]. Some years later, other researchers, by using knockout mice for the

subunit of the microprocessor complex DGCR8, found that Dgcr8−/− oocytes develop and ovulate normally, can be fertilized and give rise to viable mice [21-23]. Considering that Dicer is involved in the maturation of miRNAs and siRNAs, while DGCR8 seems to be involved only in the maturation of miRNAs, the authors concluded that miRNAs are not essential for oogenesis and embryo development in the mouse and that only siRNAs and piRNAs are likely to be active in germ cells [21-23]. The loss of function of oocyte miRNAs could be distinctive of mice, in fact, in this species an amino-terminally truncated isoform of Dicer ($Dicer^0$) is produced. $Dicer^0$ is essential for mouse oocyte functions and shows particular affinity for siRNA maturation with respect to miRNAs [24].

Further studies should address the function of miRNAs in mouse oocytes, also because maturation steps specific to individual miRNAs have been uncovered [25]. In other species miRNAs are functional and control mRNAs known to be essential for follicle growth, oocyte maturation, and embryo development [10-16].

Decreased female fertility with advanced maternal age is well documented and it is widely recognized that the decline in oocyte quality is a key phenomenon to explain infertility: it is associated with a higher risk of birth defects, genetic disorders and miscarriage [26, 27]. Several papers have investigated the transcriptome of protein encoding genes of human oocytes and its alterations related to aging, but to our knowledge, no data on miRNA expression profiles during reproductive aging has been published [28-30].

To identify human oocyte miRNAs and demonstrate that conditions altering oocyte quality, such as reproductive aging, can influence miRNA expression, we compared miRNA profiles in MII oocytes from young and old women who had undergone an in vitro fertilization program, by using a high-throughput (HT) technology. Using a computational approach, we investigated whether differentially expressed (DE) miRNAs are able to regulate pathways involved in oocyte aging. Finally, we identified evolutionary conserved miRNAs between humans and mice and their shared mRNA targets. We compared their expression profiles in old and young mice assessing, at the same time, the expression of miRNAs and mRNAs.

MATERIALS AND METHODS

Ethics

The study was approved by the Institutional Ethical Committee Catania 1 and all patients provided written informed consent. All the experiments on murine oocytes were carried out in accordance with the guidelines for the care and use of laboratory animals approved by the Animal Care Committee of the University of L'Aquila, Italy.

Patients and oocyte collection

Oocytes were donated by healthy women who had undergone intra-cytoplasmic sperm injections (ICSI) at the IVF CENTER in Cannizzaro Hospital, Catania, Italy. All patients included in this study were known to have male-dependent primary infertility. These women had no endometriosis, polycystic ovaries, ovarian insufficiency, or metabolic syndromes. Finally, heavy smokers and overweight women were excluded from the study. Our exclusion criteria were designed to avoid limiting factors in female fertility, which could affect oocyte quality. Two age categories of patients were defined: women from 38 to 40 years (older group) and women from 28 to 35 years (younger group). Our research followed the tenets of the Declaration of Helsinki. The oocytes were collected from patients who had been treated with GnRH agonists (triptorelin or buserelin), to induce multiple follicular development, followed by ovarian stimulation with

recombinant follicle stimulating hormone (rFSH) and human menopausal gonadotropin (HMG). Stimulation was monitored by serum E_2 concentrations and ultrasound measurement of follicle numbers and diameters. Ovulation was induced with 10,000 IU of human chorionic gonadotropin (HCG, Gonasi), when the dominant follicles reached 18–20 mm diameter and the serum estradiol concentration per follicle was 150−200 ng/l. Transvaginal ultrasound–guided pick-up of ovarian follicles was performed 34–36 h after hCG injection. Cumulus-enclosed oocytes were separated from follicular fluid, placed in medium and incubated for two hours at 37°C in a humidified 5% CO_2 atmosphere. After incubation, oocytes were treated with 80 IU/ml of hyaluronidase (Synvitro Hyadase; Medicult, Jyllinge, Denmark) and then rinsed three times in culture medium (ISM1 culture medium, Origio, Denmark). Special care was taken to ensure the complete lack of corona cells from oocytes, in order to select the three best MII oocytes for ICSI procedures from each patient. Oocytes were evaluated by an inverted microscope at ×200 magnification for structural parameter assessment, (zona pellucida, polar body and cytoplasm). At the end of the injection, supernumerary eggs were prepared for molecular studies, choosing those with optimal morphology. A total of 12 mature MII oocytes, six from 3 older women (old oocytes) and six from 3 younger women (young oocytes) were collected (two oocytes from each woman).

miRNA Profiling of Human Oocytes: RNA isolation, miRNA Reverse Transcription and Real Time PCR

Two MII oocytes from the same woman were placed together in an Eppendorf tube: the six samples (three from younger group and three from older group) were analyzed for the expression of 384 miRNAs by TaqMan Low Density Array (TLDAs) technology (Applied Biosystem, Foster City, CA, USA). This highly specific technology allows amplification of only mature miRNAs [31]. Each sample was rinsed several times in RNase-free water, to remove any trace of cell culture medium, and then placed in water and stored at -80°C. According to a previously published protocol, RNA from human oocytes was extracted by thermolysis: the samples were incubated for 1 min at 100°C in order to release nucleic acids [32]. Every sample was brought to a volume of 3.2 µl with water and directly reverse transcribed (RT), without prior RNA purification, using TaqMan MicroRNA Reverse Transcription Kit and Megaplex RT Primers, Human Pool A (Applied Biosystems), in a final volume of 7.5 µl. Preamplification of cDNA from 2.5 µL of RT reaction product, using Megaplex PreAmp Primers Pool A and TaqMan PreAmp Master Mix (2x) (Applied Biosystems), was run in a final volume of 25 µl. Preamplified products were diluted with 75 µl of RNase-free purified water and 18 µl were loaded on TLDAs, TaqMan Human MicroRNA Array v3.0 A (Applied Biosystems). qRT-PCR reactions were performed on a 7900HT Fast Real Time PCR System (Applied Biosystems) as follows: 94.5°C for 10 min, followed by 40 amplification cycles of 97°C for 30 s and 59.7°C for 1 min.

Expression Data Analysis

MiRNAs with a Ct lower than 37, showing optimal amplification plots, were considered as detected, while undetermined Ct values were assigned a value of 40. A miRNA, which had been detected in at least 3 of the six samples, was considered as expressed in human oocytes.
To normalize miRNA profiling data, median and average expression of the plate and the pairwise Pearson correlation (r) for all miRNAs were calculated to identify the more stable miRNAs that showed constant expression levels among individual samples. GeNorm and NormFinder statistical algorithms were used to confirm their stability and select the endogenous controls. GeNorm analysis revealed that miR-342-3p and miR-372 were the most stable, having

both the lowest average expression stability M-values (0.11). The lower the M-value, the more stably expressed are the reference genes [33]. Similarly, NormFinder indicated that the combination of miR-342-3p and miR-372, with the smallest stability value (0.005), was the best [34].

Differential expression of miRNAs between young and old oocytes was identified by Significance Analysis of Microarrays (SAM) tests (i.e., Tusher, minimum S value, the 5^{th}, 50^{th} and 90^{th} percentiles, by applying a two-class unpaired test among ΔCt and using a P value based on 100 permutations; imputation engine: K-nearest neighbors, 10 neighbors); False Discovery rate <0.30. We considered as DE only those miRNAs with two housekeeping miRNAs in common, after at least two SAM tests. The relative expression was obtained by applying the $2^{-\Delta\Delta Ct}$ method. ΔCt values were independently calculated by using miR-342-3p and miR-372 Ct mean. ΔCt means of old and young oocytes were used to determine ΔΔCt; young oocytes were chosen as calibrator. The mean fold change was calculated as a natural logarithm of RQ values; the error was estimated by evaluating the $2^{-\Delta\Delta Ct}$ equation, using ΔΔCt plus SD and ΔΔCt minus SD according to the Livak and Schmittgen method [35]. Since relative quantification with different reference miRNAs did not differ significantly and produced similar relative expression data, only RQ values obtained with the housekeeping miR-342 are shown.

In order to identify the miRNAs showing a steady expression level in every sample, we selected the miRNAs showing median and average pairwise correlation coefficients (*r*) greater than or equal to 0.75. The median of ΔCt values (by using miR-342 as the housekeeping miRNA) of old and young oocytes were used to calculate the *r* and P value, by using Statistica 10.0.

Genomics of oocyte miRNAs

Chromosome and nucleotide positions were determined by UCSC Genomic Browser (https://genome.ucsc.edu/) and the data-base Gene of NCBI (http://www.ncbi.nlm.nih.gov/gene). The sequences of mature miRNAs were retrieved from MirBase (http://mirbase.org/).

Pathway Analysis of SE miRNAs

To investigate the role of SE miRNAs the computational analysis of molecular signaling pathways, selecting for targets retrieved from Tarbase and microT-CDS, was carried out by Diana mirPath v.3 (http://snf-515788.vm.okeanos.grnet.gr/). The false discovery rate (FDR) method, as a correction for multiple hypotheses testing, was implemented to select the biological pathways with a threshold of significance defined by a P value <0.05 and a microT threshold of 0.8 [36].

Enrichment Analysis for Biological Processes and Target Gene Pathways of DE miRNAs

Validated and potential targets of DE miRNAs were searched for, using a computational approach, based on a combination of three different tools: starBase v2.0, miRTarBase v4.5 and TarBase v7.0. Enrichment analysis for biological processes and target gene pathways was performed by using protein-coding genes, associated with maturation of oocytes in humans (http://okdb.appliedbioinfo.net/) [37, 38] and expressed together in aging. A list of genes involved in the physiological aging process can be obtained from GenAge, a reliable database of genes related to aging in humans and in model organisms (http://genomics.senescence.info/genes/models.html). The final target list was then uploaded to PANTHER (Protein ANalysis THrough Evolutionary Relationships) Classification System, version 10.0: this is a comprehensive database of protein trees, families, subfamilies and

functions, available at http://pantherdb.org, which was designed to classify proteins (and their coding genes) in order to facilitate high-throughput analysis. The Gene Ontology (GO) analysis was applied to analyze the main functions of the target genes of DE miRNAs. The functional classification of miRNA targets was focused on GO experimentally observed biological process. The statistical overrepresentation test was executed and the Bonferroni correction for multiple testing was used to correct the P value. GOs with a P value <0.05 were chosen. DE miRNA target genes were subsequently used in a signaling pathway enrichment analysis in Diana-miRPath v2.0 (http://www.microrna.gr/miRPathv2). The predefined list of genes expressed in MII human oocytes and aging-related genes was uploaded to carry out pathway analysis of *in silico* predicted and experimentally validated miRNA gene targets, according to the Kyoto Encyclopedia of Genes and Genomes (KEGG). The FDR method was implemented to select the biological pathways with a threshold of significance defined by a P value <0.05 and a microT threshold of 0.8 [36].

Identification of evolutionary conserved miRNAs in humans and mice and Network analysis

Among the DE miRNAs in aged human oocytes, we identified those having the same mature sequence in humans and mice deposited in miRBase 21 (http://www.mirbase.org) and at the same time sharing the same mRNA targets. Common genes between humans and mice were screened using Diana-LAB miRNA target prediction algorithms (microT-CDS and Tarbase v7.0). A list of 7 conserved miRNAs and the 125 target genes was entered in Cytoscape version 3.2.1, for further analysis. The biological network was built by retrieving the corresponding interactome data through Cytoscape plug-in GeneMANIA v.3.4.0, selecting for physical, genetic and pathway interactions. We generated a subnetwork with 101 nodes, by taking only first neighbors between miRNAs and target genes in the network. The resulting network was analyzed using the Cytoscape plug-in CentiScaPe v.2.1, to calculate the centrality parameters of individual nodes. The conserved miRNAs were analyzed in six aliquots of murine oocytes, by single assays.

Mouse oocyte collection

For oocyte isolation, CD-1 young (4-5 weeks) and reproductively old (36 weeks) mice (very close to the end of their reproductive lifespan), were stimulated by 7.5 IU pregnant mare's serum gonadotropin (PMSG) (Folligon; Intervet-International, Boxmeer, Netherlands) to induce follicular development; 48 h later, ovulation was induced by 7.5 IU human chorionic gonadotropin (hCG) (Profasi HP 2000; Serono, Rome, Italy) [39]. All experiments were carried out in accordance with the guidelines for the care and use of laboratory animals, approved by the Animal Care Committee of the University of L'Aquila, Italy. Fifteen hours after hCG administration, oviducts were dissected from mice and cumulus-oocyte complexes (COCs) collected by puncture of the oviduct. Following dissociation of cumulus-oocyte complexes in hyaluronidase 0.1% (Sigma-Aldrich), mature oocytes arrested at metaphase II stage (MII) were isolated and pooled in groups of 30 oocytes. Three pools of oocytes from young mice and three from old mice were washed in RNase-free water, transferred to 10 µL of Trizol, placed in liquid nitrogen, and stored at −80°C until use [40].

Expression analysis of miRNAs and mRNAs in mouse oocytes

Total RNA for expression analysis was extracted by using TRIzol (Life Technologies, Monza, Italy), according to the protocol provided by the manufacturer. After quantification, 5 ng of total

RNA were used for miRNA-specific reverse transcription (RT) to obtain miRNA-specific cDNAs. Four-fifths of the cDNA total volumes were analyzed with quantitative real-time polymerase chain reaction (RT–PCR), using TaqMan MicroRNA Assays (Applied Biosystems). All real-time PCR reactions were performed in 20 µl volume, containing 10 µl of TaqMan Universal PCR Master Mix (Applied Biosystems), 1 µl of miRNA-specific TaqMan MicroRNA Assay (Applied Biosystems), 6 µl of RT product, and 3µl of nuclease-free water. We assayed seven miRNAs: let-7b-5p (Assay ID 002619), miR-19a-3p (Assay ID 000395), miR-29a-3p (Assay ID 002112), miR-126-3p (Assay ID 002228), miR-192-5p (Assay ID 000491), miR-203a-3p (Assay ID 000507), and miR-494-3p (Assay ID 002365). These assays specifically detect mature miRNAs. For each reaction, the following amplification profile was applied: 95°C for 10 min for the first cycle; 95°C for 15s and 60°C for 1 min for 40 cycles. The results were normalized to the expression level of U6 and analyzed by the ΔΔCt method.
To assess the expression of DE miRNA targets, conserved genes, resulting from network centrality analysis and selected from literature data, were analyzed. Primers of Dnmt3a (DNA Methyltransferase 3 Alpha), Dnmt3b (DNA Methyltransferase 3 Beta), Pten (Phosphatase and tensin homolog) and Tfam (Mitochondrial transcription factor A), were designed using Primer-Blast software http://www.ncbi.nlm.nih.gov/tools/primer-blast/ (Supplemental Table S1, available online at www.biolreprod.org). cDNA was synthesized from 100 ng of total RNA using SuperScript II Reverse Transcriptase (Invitrogen S.R.L., Milan, Italy) and random hexamer primers (Roche Molecular Diagnostics, Mannheim, Germany). PCR reactions were carried out by Power SYBR Green PCR Master Mix kit (Applied Biosystem) in a final volume of 20 µl containing 2 µl of cDNA. For each reaction, 40 cycles of amplification with the following profile were performed: 95°C for 10 min for the first cycle; 95°C for 15 s and 60°C for 1 min for 40 cycles; then, 95°C for 15 s and 60°C for 15 s. Relative expression levels for each gene were calculated by the ΔΔCt method, obtained by normalization of the level of each transcript to the expression of Hprt and to the normalized level of the transcript of the young oocytes used as control group.

Statistical analysis

The mean ΔCT and the standard deviation of the mean were calculated using the statistical function of Microsoft Excel 2010. Statistical significance was determined by unpaired t-test (two-tailed) from ΔCt values of the old oocytes and controls. The miRNA-target correlation was determined by the Pearson correlation test. A P value of ≤ 0.05 was considered statistically significant.

RESULTS

miRNA profiling of Human MII oocytes

Expression profiles of 384 miRNAs in 6 old and 6 young human oocytes showed that 128 miRNAs are expressed in human female germ cells. The comparison between old and young oocytes showed that 25 had steady expression levels in every sample with a coefficient of correlation $r = 0.96$, P value <0.0001 (Steadily Expressed miRNAs, SE miRNAs) (Fig. 1A). On the other hand, 12 miRNAs displayed significant expression differences in oocytes from women of advanced reproductive age (Differentially Expressed miRNAs, DE miRNAs) (Fig. 1B). Among the 12 miRNAs displaying significant expression differences with aging, we found 3 miRNAs strongly downregulated in oocytes from older women: let-7b-5p (ln RQ= -4.6 ± 0.23), miR-19a-3p (ln RQ= -3.5 ± 0.42), miR-519d-3p (ln RQ= -5.4 ± 0.23) (Fig. 1C). On the contrary,

9 miRNAs, (let-7e-5p, miR-29a-3p, miR-126-3p, miR-136-5p, miR-192-5p, miR-203a-3p, miR-371-3p, miR-484 and miR-494-3p) were upregulated (Fig. 1C). Among them, miR-192-5p and miR-203a-3p showed RQ values about 100-fold (ln RQ= 4.6 ± 1.29) and 78-fold (ln RQ= 4.3 ± 0.97) higher in old oocytes (Fig. 1C). Ninety-one miRNAs, even if detected, displayed high variability among the different samples (Table 1).
The genomics of SE and DE miRNAs reveal the presence of some clustered miRNAs (Table 2). We found 5 miRNAs of the 17-92 cluster, 3 in C14MC (Chromosome 14 MicroRNA Cluster), 3 in miR-371 cluster, 6 in C19MC (Chromosome 19 MicroRNA Cluster) and 4 in miR-106a cluster (Table 2). Six miRNAs presented a paralogous gene located in a different genomic region, sharing the same mature sequence; it was not possible to discriminate them by expression studies. Nine miRNAs shared all the AAGUGC sequences described in miRNAs involved in stemness and pluripotency [41] (Fig. 2).

Gene Target prediction, Gene Ontology and Pathway Analysis of Steadily and Differentially Expressed miRNAs

Bioinformatics analysis of SE miRNAs showed their involvement in different biological pathways; the most significant are shown in fig. 3. All 25 miRNAs are able to control *Signaling pathways regulating pluripotency of stem cells,* targeting mRNAs involved in proliferation, differentiation and regulation of the cell cycle (Fig. 3).
The 12 DE miRNAs were predicted to regulate 1,638 protein-coding genes. In order to make a more specific analysis, we interpolated these targets with specific oocyte genes and human aging-related genes: with this strategy, we reduced the number of DE miRNA targets from 1,638 to 153 (Fig. 4A). Among these 153 mRNAs, 27 could be particularly interesting because they are common between oocyte genes and aging (Fig. 4A). The GO analysis of the 153 candidate target genes showed that the following GO categories were highly and significantly represented: *regulation of gene expression*, *cell cycle process*, *chromosome organization*, *RNA metabolic process*, *response to stress*, *apoptotic process*, *chromatin modification* and *remodelling*, *response to oxygen-containing compounds*, *cell aging, cellular senescence, and signal transduction in response to DNA damage* (Fig. 4B). Candidate target genes were found to be significantly enriched in 13 KEGG pathways (P value <0.05) (Fig 4C). Notably, these include *mTOR, VEGF*, *PI3K-Akt*, *ErbB*, *Insulin*, *p53, HIF1 signaling pathways*, *Progesterone-mediated oocyte maturation*, *Endometrial cancer, Cell cycle*, *Oocyte meiosis,* and *Dorso ventral axis formation* (Fig. 4C).

Network analysis for the identification of miRNAs and mRNAs shared between humans and mice

Among the 12 DE miRNAs in aged human oocytes, we selected 7 evolutionary conserved miRNAs for sequence and functions. First of all, we identified 10 miRNAs (let-7b-5p, let-7e-5p, miR-19a-3p, miR-29a-3p, miR-126-3p, miR-136-5p, miR-192-5p, miR-203a-3p, miR-484, and miR-494-3p) as having 100% identity between humans and mice (www.mirbase.org/). Among them, 7 miRNAs (let-7b-5p, miR-19a-3p, miR-29a-3p, miR-126-3p, miR-192-5p, miR-203a-3p, and miR-494-3p) also shared orthologous target genes, thus also showing functional homology. In figure 5, we show the interactions among the 7 miRNAs and some conserved mRNAs (Fig. 5). The network, consisting of 101 nodes and 532 edges (gene relationship, pathway involvement, physical interactions), shows 51 common nodes representing human - mouse orthologous gene encoding proteins (blue circles and red diamonds). Particularly, 20 of them

(ADSS, ALCAM, BRWD1, DNMT3A, DNMT3B, EDN1, EFNB2, FOXJ2, PTEN, PURA, RAP1A, RAP1B, RBFOX2, RHOB, RICTOR, RRM2, SOCS3, STK38, TFAM, UBE2A) are important topological orthologs (red diamonds) with Degree >6.4, Betweenness >0.0042, Closeness >40.5, and Eccentricity >0.25 (Fig. 5).

Expression analysis of age-related miRNAs and their mRNA targets in mouse oocytes

The 7 miRNAs that share sequence and functional homology (yellow nodes in the network), were analyzed by single assays in mice. We found upregulation of 4 of them: mir-29a-3p (ln RQ 1.5 ± 0.29), miR-192-5p (ln RQ 1.3 ± 0.64), miR-203a-3p (ln RQ 1.8± 0.36), and miR-494-3p (ln RQ 1.5 ± 1.26) (Fig. 6). Statistical analysis confirmed that expression differences of miR-29a-3p miR-203a-3p and miR-494-3p are significant (Fig. 6). Mir-19a-3p, miR-126-3p and let-7b-5p, are expressed in murine oocytes but their expression levels do not change in aging. We selected 4 mRNAs validated targets of miR-29a, miR-203 and miR-494-3p belonging to the 20 important topological orthologs in the network (red diamonds). Specifically, Dnmt3a (miR-29a-3p target), Dnmt3b (miR-29a-3p and miR-203a-3p target), Pten (miR-29a-3p and miR-203a-3p target), and Tfam (miR-494-3p target) [42–50]. We found a significant downregulation of each messenger and demonstrated a significant negative correlation between miR-29a-3p and its targets (Dnmt3a, Dnmt3b, Pten), between miR-203a-3p and Dnmt3b, and between miR-494-3p and Tfam (Fig. 6).

DISCUSSION

Maternal RNAs represent an important store that oocytes accumulate during their growth, determine oocyte quality and establish embryo features. Several studies have focused on mRNAs, demonstrating the importance of the oocyte transcriptome, however, to date, very limited studies are available on miRNA expression profiles in human female germ cells and on their biological function. To date, non-coding RNAs are considered very important regulators of gene expression, thus, it seems logical to hypothesize that miRNAs could perform their biological role in female germ cells, during maturation or in the first phases of embryo development. Accordingly, their altered expression could lead to low quality oocytes and therefore contribute to reproductive disorders [4– 6].

In this paper, we report the identification of 128 miRNAs expressed in human oocytes (Table 1). Among them, 25 showed a steady expression in every sample (SE miRNAs), 12 were DE in oocytes from women of advanced reproductive age and 91 showed high variability among the different samples within the same group (Table 1 and Fig. 1). Among this last fraction, we found miRNAs previously identified in human oocytes (miR-10a, miR-100, miR-141, miR-212, miR-625 and miR-888) [14, 15]. The high variability of expression could depend on inter-individual differences able to influence the transcriptome, such as genetic background or life styles [9].

The 25 SE miRNAs regulate some pathways involved in basic cellular function such as *RNA transport*, *mRNA surveillance* and *regulation of the actin cytoskeleton.* Moreover, it is interesting that *signaling pathways regulating pluripotency of stem cells* is one of the most significant (Fig. 3).

The well-characterized ESC miRNome includes the miR-371–373 cluster family (the miR-290–295 cluster in the mouse), the miR-17-92 cluster and its paralogues located in the miR-106 cluster, and the miR-302/miR-467 group [41]. Most of these display the 5′-proximal AAGUGC motif that seems to be typical of Embryonic miRNAs (EmiRNAs) [41]. We found different members of the first 3 clusters steadily expressed in human oocytes (Fig. 2). We also found some

members of C19MC that is a primate specific cluster and it has been described as mainly expressed in placenta (Fig. 2) [51]. This represents the largest human cluster and we propose that some members could be classified as EmiRNAs, because we found the AAGUGC motif conserved in the four identified miRNAs (Fig. 2). Moreover, previous papers reported that some miRNAs located in this cluster are expressed in human Embryonic Stem Cells [52]. It has been reported that EmiRNAs are expressed during early mammalian development and their earliest known role is during maternal–zygotic transition (MZT), when zygotic transcription starts and maternal mRNAs are degraded [41, 53]. We may propose that SE miRNAs are part of the maternal storage of essential RNAs, which oocytes synthesize during their growth and perform their role during the first phase of embryo development. Similar to pluripotential factors Oct3/4, Sox2, Klf4, and c-Myc expressed in human oocytes, these miRNAs could represent the oocyte store able to reprogram the nucleus of somatic cells. If oocytes are devoid of this storage, they are not able to produce a vital embryo. Therefore, these miRNAs represent molecular markers of oocyte quality.

Stronger data, suggesting an active role of miRNAs in human oocytes, report that some of them showed altered expression in reproductive aging, a condition that causes a reduction of reproductive efficiency and alters oocyte quality by modifying gene expression [26-30]. We found 12 DE miRNAs in oocytes from women of advanced reproductive age and by bioinformatics analysis we demonstrated that DE miRNAs contribute to the alteration of oocyte pathways which is characteristic in aging [28-30, 54-56]. The functional role of miRNA targets in human oocytes was accurately evaluated and a comprehensive computational analysis of deregulated miRNAs in oocyte aging was performed. One of the main problems of miRNA target prediction tools is that the software retrieves all mRNAs able to be regulated by input miRNAs without making a selection based on tissue specificity or particular functions. This means that a lot of messengers are retrieved and further analysis, based on these predictions, lacks specificity. To avoid this problem, we performed an enrichment analysis and out of 1,638 mRNA targets identified initially, we selected 153 mRNAs representing specific oocyte genes and human aging-related genes (Fig. 4A). Based on these 153 targets, identified GO terms overlapped to GO categories previously identified by studying mRNAs deregulated in oocyte aging (Fig. 4B) [28-30, 54-56]. We found genes related to cell cycle, chromosome organization, stress response, DNA stability, modulation of chromatin architecture, management of oxygen, the response to DNA damage and regulation of the apoptotic process, which have been described to be altered by age, in mouse and human metaphase II oocytes (Fig. 4B) [28, 30, 54]. Pathway analysis identified genes involved in oocyte maturation (*Progesterone-mediated oocyte maturation, mTOR, PI3K-AKT,* and *ErbB signaling pathways*) and pinpointed the major pathways involved in aging (*P53, mTOR,* and *cell cycle signaling pathways*), in agreement with previously published papers (Fig. 4C) [29, 55]. These data confirmed that the identified miRNAs are involved in oocyte aging.

The strategies used to control gene expression have many similarities between humans and mice, even if mouse oocytes do not necessarily represent an ideal model to study the regulation of gene expression carried out by miRNAs. Moreover, in our study we found different members of primate specific cluster C19MC expressed in human oocytes and absent in the mouse [51]. Nevertheless, the mouse model could represent a good alternative and could be used to confirm human data because of poor availability of human oocytes. We drew a network showing the molecular interaction among the 7 conserved miRNAs (let-7b-5p, miR-19a-3p, miR-29a-3p, miR-126-3p, miR-192-5p, miR-203a-3p, and miR-494-3p) and their target genes came out from

identified by the enrichment analysis. In the network, we identified, in addition to human specific targets (black circles), orthologous genes (blue circles and red diamonds) and among these the most central nodes (red diamonds) (Fig. 5). This network could represent a starting point for translating results from mice to humans.

We analyzed the 7 conserved miRNAs in mouse oocytes and we confirmed the upregulation of miR-29a-3p, miR-203a-3p, and miR-494-3p in old ones.

Integrating centrality results with literature data, we selected Dnmt3a, Dnmt3b, Pten, and Tfam (central nodes and validated targets of miR-29a-3p, miR-203a-3p, and miR-494-3p) and analyzed their expression in the same aliquots of mouse oocytes. We found the corresponding downregulation of all mRNAs (Fig. 6).

It has been demonstrated in different cellular models that miR-29a and miR-203 regulate *de novo* DNMT3A and DNMT3B in humans and mice [42, 49, 57].

DNA methylation is an epigenetic mechanism essential for chromatin remodeling and regulation of gene expression in mammals. It is important for embryonic development, imprinting, X-chromosome inactivation and the maintenance of genome stability by the repression of retrotransposons [58]. Dnmt3a and Dnmt3b are responsible for *de novo* methylation and play critical roles during gametogenesis and, above all, in early development [59-62]. During the oocyte growth phase, before meiosis resumption, DNMT3s establish the oocyte methylation patterns and mark a subset of genes for activity in the embryo, such as imprinted genes [59, 60]. During the early phases of embryo development, subsequent to demethylation waves needed for genome reprogramming and to reach the totipotent state, *de novo* methylation contributes to the first lineage specification allowing the differentiation between trophoectoderm and inner cell mass [61, 62]. The aging phenotype is influenced by epigenetic modifications, alteration of DNA methylation increases with increasing age and may predispose to age-associated diseases [63]. Also in reproductive biology, alteration of DNA methylation levels related to aging has been seen in oocytes and pre-implantation embryos [64]. Genome-wide DNA methylation is lower in 35- to 40-week-old mouse oocytes and also DNMT expression is decreased in aged oocytes [54, 65, 66]. Moreover, it has been shown that their decreasing expression may be related to a lower reproductive potential in old female mice and in human oocytes altered expression of DNMT3B is associated with low oocyte quality [66, 67].

We found miR-29a-3p and miR-203a-3p upregulated in old human and mouse oocytes and we demonstrated, in the mouse model, that their overexpression correlates with Dnmt3a and Dnmt3b downregulation (Fig. 3 and Fig. 5). According to literature data, we found the downregulation of Dnmt3s in aging and identified human and mouse oocyte miRNAs involved in their altered regulation. The identification of miRNAs regulating DNMT3s in oocytes could open up the possibility to improve oocyte quality in aging and also in reproductive disorders [68, 69].

PTEN, validated target of miR-29a-3p and miR-494-3p, is an indispensable molecule that maintains the dormancy of the primordial follicle pool inhibiting the phosphatidylinositol 3-kinase (PI3K) signaling pathway [44, 45, 70, 71]. Its downregulation represents an important step in the cyclical activation of primordial follicles. The depletion of the primordial follicle pool leads to the end of female reproductive life and it has been demonstrated that in mice lacking Pten the entire primordial follicle pool becomes activated causing Premature Ovarian Failure [70]. The significant downregulation of Pten found in older oocytes could be closely associated with the decrease of ovarian reserve, a hallmark of aging [71]. In addition, the PI3K pathway is involved in other steps of follicular maturation: acting in granulose cells, it regulates cyclic follicular recruitment and ovulation, while it stimulates meiosis resumption in oocytes [72]. The

modulation of PTEN levels, inside ovarian follicles, requires a fine regulation that could be carried out by miR-29a-3p and miR-494-3p [73]. Moreover, their overexpression and the resulting PTEN downregulation related to aging could have a negative effect on the embryo because it has been seen that PTEN is essential for embryonic development [74]. Our data showed a significant upregulation of miR-494-3p associated to the downregulation of Tfam in older oocytes. The TFAM gene encodes a key mitochondrial transcription factor and it is able to regulate the mtDNA copy number [75]. It has been demonstrated that miR-494-3p is able to regulate mitochondrial biogenesis by downregulating TFAM during myocyte differentiation and skeletal muscle adaptation to physical exercise [47]. TFAM is expressed in mammalian oocytes. It has been shown that expression of mRNAs is higher in human MII oocytes compared with GV and MI ones and a recent study has displayed that bovine oocytes with low developmental competence and cleavage failure exhibit a lower expression of TFAM [76-79]. The miR-494 upregulation in old human and mouse oocytes related to downregulation of TFAM could explain the lower number of mitochondria associated with oocyte aging [80, 81].
We characterized miRNA profiles in human oocytes identifying the expression differences in reproductive aging. These data advance our knowledge on the oocyte trascriptome and represent the first step to improve prognosis, diagnosis and eventually therapy in reproductive medicine.

ACKNOWLEDGEMENTS
The authors would like to thank Danila Santagati and Desirè Arena, undergraduate students, for their involvement in this project and the Scientific Bureau of the University of Catania for language support.

REFERENCES
1. ENCODE Project Consortium. An integrated encyclopedia of DNA elements in the human genome. Nature 2012; 489: 57-74.
2. Djebali S, Davis CA, Merkel A, Dobin A, Lassmann T, Mortazavi A,Tanzer A, Lagarde J, Lin W, Schlesinger F, Xue C, Marinov GK, et al. Landscape of transcription in human cells. Nature 2012; 489: 101-108.
3. Fu XD. Non-coding RNA: a new frontier in regulatory biology. Natl Sci Rev 2014; 1: 190-204.
4. Bartel DP. MicroRNAs: genomics, biogenesis, mechanism, and function. Cell 2004; 116: 281-297.
5. Virant-Klun I, Ståhlberg A, Kubista M, Skutella T. MicroRNAs: From Female Fertility, Germ Cells, and Stem Cells to Cancer in Humans. Stem Cells Int 2016; 2016: 3984937.
6. Croce CM. Causes and consequences of microRNA dysregulation in cancer. Nat Rev Genet 2009; 10: 704-714.
7. McGinnis LK, Luense LJ, Christenson LK. MicroRNA in Ovarian Biology and Disease. Cold Spring Harb Perspect Med 2015; 5(9):a022962.
8. Zuccotti M, Merico V, Cecconi S, Redi CA, Garagna S. What does it take to make a developmentally competent mammalian egg? Hum Reprod Update 2011; 17(4):525-540.
9. Labrecque R, Sirard MA. The study of mammalian oocyte competence by transcriptome analysis: progress and challenges. Mol Hum Reprod 2014; 20:103-116.
10. Giraldez AJ, Mishima Y, Rihel J, Grocock RJ, Van Dongen S, Inoue K et al. Zebrafish MiR-430 promotes deadenylation and clearance of maternal mRNAs. Science 2006; 312: 75-79.
11. Abramov R, Fu G, Zhang Y, Peng C. Expression and regulation of miR-17a and miR-430b in

zebrafish ovarian follicles. Gen Comp Endocrinol 2013; 188:309-315.
12. Cui XS, Sun SC, Kang YK, Kim NH. Involvement of microRNA-335-5p in cytoskeleton dynamics in mouse oocytes. Reprod Fertil Dev 2013; 25:691-699.
13. Gilchrist GC, Tscherner A, Nalpathamkalam T, Merico D, LaMarre J. MicroRNA Expression during Bovine Oocyte Maturation and Fertilization. Int J Mol Sci 2016; 17:396.
14. Xu YW, Wang B, Ding CH, Li T, Gu F, Zhou C. Differentially expressed micoRNAs in human oocytes. J Assist Reprod Genet 2011; 28:559-566.
15. Assou S, Al-edani T, Haouzi D, Philippe N, Lecellier CH, Piquemal D, et al. MicroRNAs: new candidates for the regulation of the human cumulus-oocyte complex. Hum Reprod 2013; 28: 3038-3049.
16. Tulay P, Naja RP, Cascales-Roman O, Doshi A, Serhal P, SenGupta SB. Investigation of microRNA expression and DNA repair gene transcripts in human oocytes and blastocysts. J Assist Reprod Genet 2015; 32: 1757-1764.
17. Tam OH, Aravin AA, Stein P, Girard A, Murchison EP, Cheloufi S, Hodges E, Anger M, Sachidanandam R, Schultz RM, Hannon GJ. Pseudogene-derived small interfering RNAs regulate gene expression in mouse oocytes. Nature 2008; 453: 534-538.
18. Watanabe T, Totoki Y, Toyoda A, Kaneda M, Kuramochi-Miyagawa S, Obata Y, Chiba H, Kohara Y, Kono T, Nakano T, Surani MA, Sakaki Y, et al. Endogenous siRNAs from naturally formed dsRNAs regulate transcripts in mouse oocytes. Nature 2008; 453: 539-543.
19. Tang F, Kaneda M, O'Carroll D, Hajkova P, Barton SC, Sun YA, Lee C, Tarakhovsky A, Lao K, Surani MA. Maternal microRNAs are essential for mouse zygotic development. Genes Dev 2007; 21:644-648.
20. Murchison EP, Stein P, Xuan Z, Pan H, Zhang MQ, Schultz RM, Hannon GJ. Critical roles for Dicer in the female germline. Genes Dev 2007; 21: 682-693.
21. Suh N, Baehner L, Moltzahn F, Melton C, Shenoy A, Chen J, Blelloch R. MicroRNA function is globally suppressed in mouse oocytes and early embryos. Curr Biol 2010; 20: 271-277.
22. Ohnishi Y, Totoki Y, Toyoda A, Watanabe T, Yamamoto Y, Tokunaga K, Sakaki Y, Sasaki H, Hohjoh H. Small RNA class transition from siRNA/piRNA to miRNA during pre-implantation mouse development. Nucleic Acids Res 2010; 38: 5141-5151.
23. Svoboda P. Why mouse oocytes and early embryos ignore miRNAs? RNA Biol 2010; 7: 559-563.
24. Flemr M, Malik R, Franke V, Nejepinska J, Sedlacek R, Vlahovicek K, Svoboda P. A retrotransposon-driven dicer isoform directs endogenous small interfering RNA production in mouse oocytes. Cell 2013; 155:807-816.
25. Winter J, Jung S, Keller S, Gregory RI, Diederichs S. Many roads to maturity: microRNA biogenesis pathways and their regulation. Nat Cell Biol 2009; 11:228-234.
26. Tatone C, Amicarelli F, Carbone MC, Monteleone P, Caserta D, Marci R, Artini PG, Piomboni P, Focarelli R. Cellular and molecular aspects of ovarian follicle ageing. Hum Reprod Update 2008; 14: 131-142.
27. Hunt PA, Hassold TJ. Human female meiosis: what makes a good egg go bad? Trends Genet 2008; 24: 86-93.
28. Grøndahl ML, Yding Andersen C, Bogstad J, Nielsen FC, Meinertz H, Borup R. Gene expression profiles of single human mature oocytes in relation to age. Hum Reprod 2010; 25: 957-968.
29. Guglielmino MR, Santonocito M, Vento M, Ragusa M, Barbagallo D, Borzì P, Casciano I,

Banelli B, Barbieri O, Astigiano S, Scollo P, Romani M, et al. TAp73 is downregulated in oocytes from women of advanced reproductive age. Cell Cycle 2011; 10: 3253-3256.
30. Santonocito M, Guglielmino MR, Vento M, Ragusa M, Barbagallo D, Borzì P, Casciano I, Scollo P, Romani M, Tatone C, Purrello M, Di Pietro C. The apoptotic transcriptome of the human MII oocyte: characterization and age-related changes. Apoptosis 2013; 18: 201-211.
31. Chen C, Ridzon DA, Broomer AJ, Zhou Z, Lee DH, Nguyen JT, et al. Real-time quantification of microRNAs by stem–loop RT–PCR. Nucleic Acids Res 2005; 33:e179.
32. Di Pietro C, Vento M, Ragusa M, Barbagallo D, Guglielmino MR, Maniscalchi T, Duro LR, Tomasello L, Majorana A, De Palma A, Borzì P, Scollo P, et al. Expression analysis of TFIID in single human oocytes: new potential molecular markers of oocyte quality. Reprod Biomed Online 2008; 17: 338-349.
33. Vandesompele J, De Preter K, Pattyn F, Poppe B, Van Roy N, De Paepe A, Speleman F. Accurate normalization of real-time quantitative RT-PCR data by geometric averaging of multiple internal control genes. Genome Biol. 2002; 3:RESEARCH0034.
34. Rho HW, Lee BC, Choi ES, Choi IJ, Lee YS, Goh SH. Identification of valid reference genes for gene expression studies of human stomach cancer by reverse transcription-qPCR. BMC Cancer. 2010; 10:240.
35. Livak KJ, Schmittgen TD. Analysis of relative gene expression data using real-time quantitative PCR and the 2(−delta deltaC(T)) method. Methods 2001; 25: 402–408.
36. Benjamini Y and Hochberg Y. A direct approach to false discovery rates. JR Stat. Soc., B, 1995, 57: 289-300.
37. Piras V, Tomita M, Selvarajoo K. Transcriptome-wide variability in single embryonic development cells. Sci Rep 2014; 4: 7137.
38. Kocabas AM, Crosby J, Ross PJ, Otu HH, Beyhan Z, Can H, et al. The transcriptome of human oocytes. Proc Natl Acad Sci U S A 2006; 103: 14027-14032.
39. Di Emidio G, Falone S, Vitti M, D'Alessandro AM, Vento M, Di Pietro C, Amicarelli F, Tatone C. SIRT1 signalling protects mouse oocytes against oxidative stress and is deregulated during aging. Hum Reprod. 2014; 29:2006-2017.
40. Tatone C, Carbone MC, Gallo R, DelleMonache S, Di Cola M, Alesse E, Amicarelli F. Age-associated changes in mouse oocytes during postovulatory in vitro culture: possible role for meiotic kinases and survival factor BCL2. Biol Reprod. 2006; 74:395-402.
41. Svoboda P, Flemr M. The role of miRNAs and endogenous siRNAs in maternal-to-zygotic reprogramming and the establishment of pluripotency. EMBO Rep. 2010;11:590-597.
42. Fabbri M, Garzon R, Cimmino A, Liu Z, Zanesi N, Callegari E, et al. MicroRNA-29 family reverts aberrant methylation in lung cancer by targeting DNA methyltransferases 3A and 3B. Proc Natl Acad Sci U S A 2007; 104:15805-15810.
43. Garzon R, Liu S, Fabbri M, Liu Z, Heaphy CE, Callegari E, Schwind S, Pang J, Yu J, Muthusamy N, Havelange V, Volinia S, et al. MicroRNA-29b induces global DNA hypomethylation and tumor suppressor gene reexpression in acute myeloid leukemia by targeting directly DNMT3A and 3B and indirectly DNMT1. Blood 2009; 113: 6411-6418.
44. Liu L, Jiang Y, Zhang H, Greenlee AR, Han Z. Overexpressed miR-494 down-regulates PTEN gene expression in cells transformed by anti-benzo(a)pyrene-trans-7,8-dihydrodiol-9,10-epoxide. Life Sci 2010; 86:192-198.
45. Kong G, Zhang J, Zhang S, Shan C, Ye L, Zhang X. Upregulated microRNA-29a by hepatitis B virus X protein enhances hepatoma cell migration by targeting PTEN in cell culture model. PLoS One 2011; 6: e19518.

46. Sandhu R, Rivenbark AG, Coleman WB. Loss of post-transcriptional regulation of DNMT3b by microRNAs: a possible molecular mechanism for the hypermethylation defect observed in a subset of breast cancer cell lines. Int J Oncol 2012; 41:721-732.
47. Yamamoto H, Morino K, Nishio Y, Ugi S, Yoshizaki T, Kashiwagi A, Maegawa H. MicroRNA-494 regulates mitochondrial biogenesis in skeletal muscle through mitochondrial transcription factor A and Forkhead box j3. Am J Physiol Endocrinol Metab 2012; 303: E1419-1427.
48. Wang J, Wang Y, Wang Y, Ma Y, Lan Y, Yang X. Transforming growth factor β-regulated microRNA-29a promotes angiogenesis through targeting the phosphatase and tensin homolog in endothelium. J Biol Chem 2013; 288:10418-10426.
49. GasqueSchoof CR, Izzotti A, Jasiulionis MG, VasquesLdos R. The Roles of miR-26, miR-29, and miR-203 in the Silencing of the Epigenetic Machinery during Melanocyte Transformation. Biomed Res Int 2015; 2015:634749.
50. Hu W, Dooley J, Chung SS, Chandramohan D, Cimmino L, Mukherjee S, Mason CE, de Strooper B, Liston A, Park CY. miR-29a maintains mouse hematopoietic stem cell self-renewal by regulating Dnmt3a. Blood 2015; 125:2206-2216.
51. Donker RB, Mouillet JF, Chu T, Hubel CA, Stolz DB, Morelli AE, Sadovsky Y. The expression profile of C19MC microRNAs in primary human trophoblast cells and exosomes. Mol Hum Reprod 2012; 18: 417-424.
52. Bar M, Wyman SK, Fritz BR, Qi J, Garg KS, Parkin RK, Kroh EM, Bendoraite A, Mitchell PS, Nelson AM, Ruzzo WL, Ware C, et al. MicroRNA discovery and profiling in human embryonic stem cells by deep sequencing of small RNA libraries. Stem Cells 2008; 26:2496-2505.
53. Pauli A, Rinn JL, Schier AF. Non-coding RNAs as regulators of embryogenesis. Nat Rev Genet 2011; 12:136-149.
54. Hamatani T, Falco G, Carter MG, Akutsu H, Stagg CA, Sharov AA, Dudekula DB, VanBuren V, Ko MS. Age-associated alteration of gene expression patterns in mouse oocytes. Hum Mol Genet 2004; 13: 2263-2278.
55. Eichenlaub-Ritter U. Oocyte ageing and its cellular basis. Int J DevBiol 2012; 56: 841-852.
56. Qian Y, Tu J, Tang NL, Kong GW, Chung JP, Chan WY, Lee TL. Dynamic changes of DNA epigenetic marks in mouse oocytes during natural and accelerated aging. Int J Biochem Cell Biol 2015; 67: 121-127.
57. Filkowski JN, Ilnytskyy Y, Tamminga J, Koturbash I, Golubov A, Bagnyukova T, Pogribny IP, Kovalchuk O. Hypomethylation and genome instability in the germline of exposed parents and their progeny is associated with altered miRNA expression. Carcinogenesis 2010; 31:1110-1115.
58. Messerschmidt DM, Knowles BB, Solter D. DNA methylation dynamics during epigenetic reprogramming in the germline and preimplantation embryos. Genes Dev 2014; 28:812-828.
59. Lucifero D, La Salle S, Bourc'his D, Martel J, Bestor T, Trasler J. Coordinate regulation of DNA methyltransferase expression during oogenesis. BMC Dev Biol 2007;7:36.
60. Tomizawa S, Nowacka-Woszuk J, Kelsey G. DNA methylation establishment during oocyte growth: mechanisms and significance. Int J Dev Biol 2012; 56:867-875.
61. Watanabe D, Suetake I, Tada T, Tajima S. Stage- and cell-specific expression of Dnmt3a and Dnmt3b during embryogenesis. Mech Dev 2002; 118:187–190.
62. Marcho C, Cui W1 Mager J. Epigenetic dynamics during preimplantation development. Reproduction 2015; 150:R109-120.

63. Ben-Avraham D, Muzumdar RH, Atzmon G. Epigenetic genome-wide association methylation in aging and longevity. Epigenomics 2012; 4: 503-509.
64. Ge ZJ, Schatten H, Zhang CL, Sun QY. Oocyte ageing and epigenetics. Reproduction 2015; 149: R103-114.
65. Lopes FL, Fortier AL, Darricarrère N, Chan D, Arnold DR, Trasler JM. Reproductive and epigenetic outcomes associated with aging mouse oocytes. Hum Mol Genet 2009; 18: 2032-2044.
66. Yue MX, Fu XW, Zhou GB, Hou YP, DU M, Wang L, Zhu SE. Abnormal DNA methylationin oocytes could be associated with a decrease in reproductive potential in old mice. J Assist Reprod Genet 2012; 29:643-650.
67. Petrussa L, Van de Velde H, De Rycke M. Dynamic regulation of DNA methyltransferases in human oocytes and preimplantation embryos after assisted reproductive technologies. Mol Hum Reprod 2014; 20:861-874.
68. Miao YL, Kikuchi K, Sun QY, Schatten H. Oocyte aging: cellular and molecular changes, developmental potential and reversal possibility. Hum Reprod Update 2009; 15: 573-585.
69. Foulks JM, Parnell KM, Nix RN, Chau S, Swierczek K, Saunders M, et al. Epigenetic drug discovery: targeting DNA methyltransferases. J Biomol Screen 2012; 17:2-17.
70. Reddy P, Liu L, Adhikari D, Jagarlamudi K, Rajareddy S, ShenY,et al. Oocyte-specific deletion of Pten causes premature activation of the primordial follicle pool. Science 2008; 319:611-613.
71. Reddy P, Adhikari D, Zheng W, Liang S, Hämäläinen T, Tohonen V, Ogawa W, Noda T, Volarevic S, Huhtaniemi I, Liu K. PDK1 signaling in oocytes controls reproductive aging and life span by manipulating the survival of primordial follicles. Hum Mol Genet 2009; 18:2813-2824.
72. Zheng W, Nagaraju G, Liu Z, Liu K. Functional roles of the phosphatidylinositol 3-kinases (PI3Ks) signaling in the mammalian ovary. Mol Cell Endocrinol 2012; 356:24-30.
73. Di Pietro C. Exosome-mediated communication in the ovarian follicle. J Assist Reprod Genet 2016; 33:303-311.
74. Di Cristofano A, Pesce B, Cordon-Cardo C, Pandolfi PP. Pten is essential for embryonic development and tumour suppression. Nat Genet 1998; 19:348-355.
75. Campbell CT, Kolesar JE, Kaufman BA. Mitochondrial transcription factor A regulates mitochondrial transcription initiation, DNA packaging, and genome copy number. Biochim Biophys Acta 2012; 1819: 921-929.
76. Mahrous E, Yang Q, Clarke HJ Regulation of mitochondrial DNA accumulation during oocyte growth and meiotic maturation in the mouse. Reproduction 2012; 144:177-185.
77. Novin MG, Allahveisi A, Noruzinia M, Farhadifar F, Yousefian E, Fard AD, Salimi M. The relationship between transcript expression levels of nuclear encoded (TFAM, NRF1) and mitochondrial encoded (MT-CO1) genes in single human oocytes during oocyte maturation. Balkan J Med Genet 2015; 18:39-46.
78. Opiela J, Lipin´ski D, Słomski R, Kataska-Ksiazkiewicz Transcript expression of mitochondria related genes is correlated with bovine oocyte selection by BCB test. Anim Reprod Sci 2010; 118: 188–193.
79. Ferreira RM, Chiaratti MR, Macabelli CH, Rodrigues CA, Ferraz ML,Watanabe YF, Smith LC, Meirelles FV, Baruselli PS. The Infertility of Repeat-Breeder Cows During Summer Is Associated with Decreased Mitochondrial DNA and Increased Expression of Mitochondrial and Apoptotic Genes in Oocytes. Biol Reprod 2016; 94:66.

80. Santos TA, El Shourbagy S, St John JC. Mitochondrial content reflects oocyte variability and fertilization outcome. Fertil Steril 2006; 85: 584-591.
81. Babayev E, Seli E. Oocyte mitochondrial function and reproduction.Curr Opin Obstet Gynecol 2015; 27:175-181.

FIGURE LEGENDS

Figure 1. Comparison of miRNA expression in old and young human oocytes. A) Scatter plot showing correlation between ΔCt values of 25 Steadily Expressed (SE) miRNAs for old and young oocytes; r value = 0.9568; P value <0.0001. **B**) Box and whisker plot of ΔCt of miRNAs with statistically significant expression differences (SAM, two-class unpaired test; False Discovery Rate <0.30) in old and young oocytes. Values on the y-axis are reported as (–)ΔCt. Boxes represent the 25th, 50th, and 75th percentile (horizontal lines).Whiskers denote maximum and minimum ΔCt values. **C**) Expression fold change of 12 Differentially Expressed (DE) miRNAs in old oocytes compared with young oocytes. Relative miRNA expression levels on the y-axis are reported as the natural logarithm of RQ values, which were calculated by the 2–ΔΔCt method (using miR-342 as an endogenous control and young oocytes as calibrator samples) and respective SD values.

Figure 2. Genomic organization of miRNA clusters. The figure shows miRNAs identified in human oocytes (grey boxes) within the 17-92, C14MC, miR-371 and C19MC clusters; the white boxes indicate undetected miRNAs. Most mature miRNAs conserve the AAGUGC motif (in black and bold). In the C19MC cluster only a few miRNAs are shown.

Figure 3. Pathway analysis for SE miRNAs. Significant KEGG pathways regulated by 25 Steadily Expressed miRNAs (SE miRNAs). The results were sorted by the number of miRNAs (y-axis), the number of target genes in each pathway (above gray bars) and the significance as -log10 (P value), (secondary vertical axis). The genes shown in the grey box represent essential targets for regulation of pathways that govern pluripotency in embryonic stem cells.

Figure 4. Target prediction, GO and pathway enrichment analysis for DE miRNAs with age. A) Venn diagram showing the overlap between miRNA targets and the number of genes that were identified in oocytes and related to aging. Targets that overlapped these 3 different data sets are listed (126 in green box and 27 in orange box). **B**) Significant GOs, in terms of experimentally observed Biological Processes, for DE miRNAs identified in human MII oocytes, are shown. The x-axis represents the -log10 (P value); the significance was determined by the adjusted Bonferroni correction. **C**) Signaling pathway heat map regulated by DE miRNAs. Pathway enrichment analysis with KEGG against listed target genes identifies the potential role of miRNA in reproductive aging. The probability values are reported as -log10 (P value). Gray boxes indicate that the pathway is not significant.

Figure 5. Regulatory network of evolutionary conserved DE miRNAs and their target genes. Interaction network consisting of conserved miRNAs (yellow circles), common target genes that are human and mouse orthologs (blue circles and red diamonds) and human target genes (black circles). Twenty key target genes (red diamonds) are strong central candidates of miRNA regulation in reproductive aging. The miRNA-mRNA network was generated by the Cytoscape tool.

Figure 6. MiRNA and mRNA expression in young and old mouse oocytes. Histograms showing expression changes of candidate miRNAs in CD-1 reproductively young (4-5 weeks) and reproductively old (36 weeks) mice. Relative expression, as the natural logarithm of RQ values ± SD, of miRNAs (grey bars) and targets (white bars), in older oocytes compared with young controls, are reported on the y-axis.* $P \leq 0.05$; ** $P \leq 0.01$ by Student's t-test. Pearson correlation (*r*) values among miRNAs and mRNA targets in mouse oocytes and the relative P values are indicated.

TABLE 1. MicroRNA profiling in human MII oocytes.

Unsteadily expressed	Steadily expressed		Differentially expressed in reproductive aging	
let-7c, miR-9, miR-10a, miR-15b, miR-18a, miR-21, miR-24, miR-26a, miR-26b, miR-28, miR-95, miR-99b, miR-100, miR-103, miR-106b, miR-125a-5p, miR-125b, miR-130b, miR-132, miR-133a, miR-135a, miR-135b, miR-138, miR-140-3p, miR-141, miR-142-3p, miR-145, miR-146b, miR-149, miR-150, miR-155, miR-182, miR-193b, miR-194, miR-195, miR-197, miR-200c, miR-202, miR-204, miR-212, miR-218, miR-222, miR-223, miR-296, miR-301, miR-323-3p, miR-328, miR-331, miR-335, miR-339-3p, miR-340, miR-345, miR-362, miR-362-3p, miR-363, miR-365, miR-422a, miR-425-5p, miR-449, miR-454, miR-487a, miR-489, miR-490, miR-500, miR-502-3p, miR-508, miR-509-5p, miR-512-3p, miR-515-5p, miR-517a, miR-518d, miR-518e, miR-518f, miR-519c, miR-520d-5p, miR-523, miR-532-3p, miR-548a, miR-548c, miR-548c-5p, miR-574-3p, miR-576-3p, miR-590-5p, miR-625, miR-628-5p, miR-671-3p, miR-885-5p, miR-886-3p, miR-886-5p, miR-888, miR-891a	1	miR-16	1	let-7b
	2	miR-17	2	let-7e
	3	miR-19b,	3	miR-19a
	4	miR-20a	4	miR-29a
	5	miR-28-3p	5	miR-126
	6	miR-20b	6	miR-136
	7	miR-30b	7	miR-192
	8	miR-30c	8	miR-203
	9	miR-31	9	miR-371a-3p
	10	miR-92a	10	miR-484
	11	miR-106a	11	miR-494
	12	miR-146a	12	miR-519d
	13	miR-184		
	14	miR-191		
	15	miR-320		
	16	miR-342-3p		
	17	miR-372		
	18	miR-373		
	19	miR-374		
	20	miR-483-5p		
	21	miR-517c		
	22	miR-518a-3p		
	23	miR519a		
	24	miR-532		
	25	miR-618		

TABLE 2. Genomics of oocyte microRNAs.

MicroRNA	Chromosome	Position	Cluster	Host gene
miR-30c-1	1p34.2	40757284 - 40757372	miR-30e/30c	NFYC
miR-191	3p21.31	49020618 - 49020709, complement	miR-191/425	DALRD3
miR-16-2	3q25.33	160404745 - 160404825	miR-15b/16-2	SMC4
miR-28	3q28	188688781 - 188688866		LPP
miR-146a	5q34	160485352 - 160485450		
miR-30c-2	6q13	71376960 - 71377031, complement		
miR-29a	7q32.3	130876747 - 130876810, complement	miR-29b-1/29a	
miR-320	8p21.3	22244962 - 22245043, complement		
miR-30b	8q24.22	134800520 - 134800607, complement	miR-30d/30b	
miR-31	9p21.3	21512115 - 21512185, complement		
miR-126	9q34.3	136670602 - 136670686		EGFL7
miR-483	11p15.5	2134134 - 2134209, complement		IGF2
miR-192	11q13.1	64891137 - 64891246, complement	miR-6750/192	
miR-618	12q21.31	80935736 - 80935833, complement		LIN7A
miR-16-1	13q14.2	50048973 - 50049061, complement	miR-15a/16-1	DLEU2
miR-17	13q31.3	91350605 - 91350688	miR-17/92a	
miR-19b-1		91351192 - 91351278		
miR-20a		91351065 - 91351135		
miR-92a-1		91351314 - 91351391		
miR-19a		91350891 - 91350972		
miR-342	14q32.2-q32.31	100109655 - 100109753	C14MC	EVL
miR-136		100884702 - 100884783		RTL1
miR-494		101029634 - 101029714		
miR-203	14q32.33	104117405 - 104117514	miR-203a/203b	
miR-184	15q25.1	79209788 - 79209871		
miR-484	16p13.11	15643294 - 15643372		NDE1
let-7e	19q13.41	51692786 - 51692864	miR- 99b/let-7e/125a	
miR-371a	19q13.42	53787675 - 53787741	miR-371a/373	
miR-372		53787890 - 53787956		
miR-373		53788705 - 53788773		
miR-517c	19q13.42	53741313 - 53741407	C19MC	
miR-518a-1		53731006 - 53731090		
miR-518a-2		53739333 - 53739419		
miR-519a-1		53752397 - 53752481		
miR-519a-2		53762344 - 53762430		
miR-519d		53713347 - 53713434		
let-7b	22q13.31	46113686 - 46113768	Let-7a-3/miR-4763/let-7b	
miR-532	Xp11.23	50003148 - 50003238	miR-532/502	CLCN5
miR-374a	Xq13.2	74287286 - 74287357, complement	miR-545/374a	FTX, XIST regulator
miR-106a	Xq26.2	134170198 - 134170278, complement	miR-106a/363	
miR-20b		134169809 - 134169877, complement		
miR-19b-2		134169671 - 134169766, complement		
miR-92a-2		134169538 - 134169612, complement		

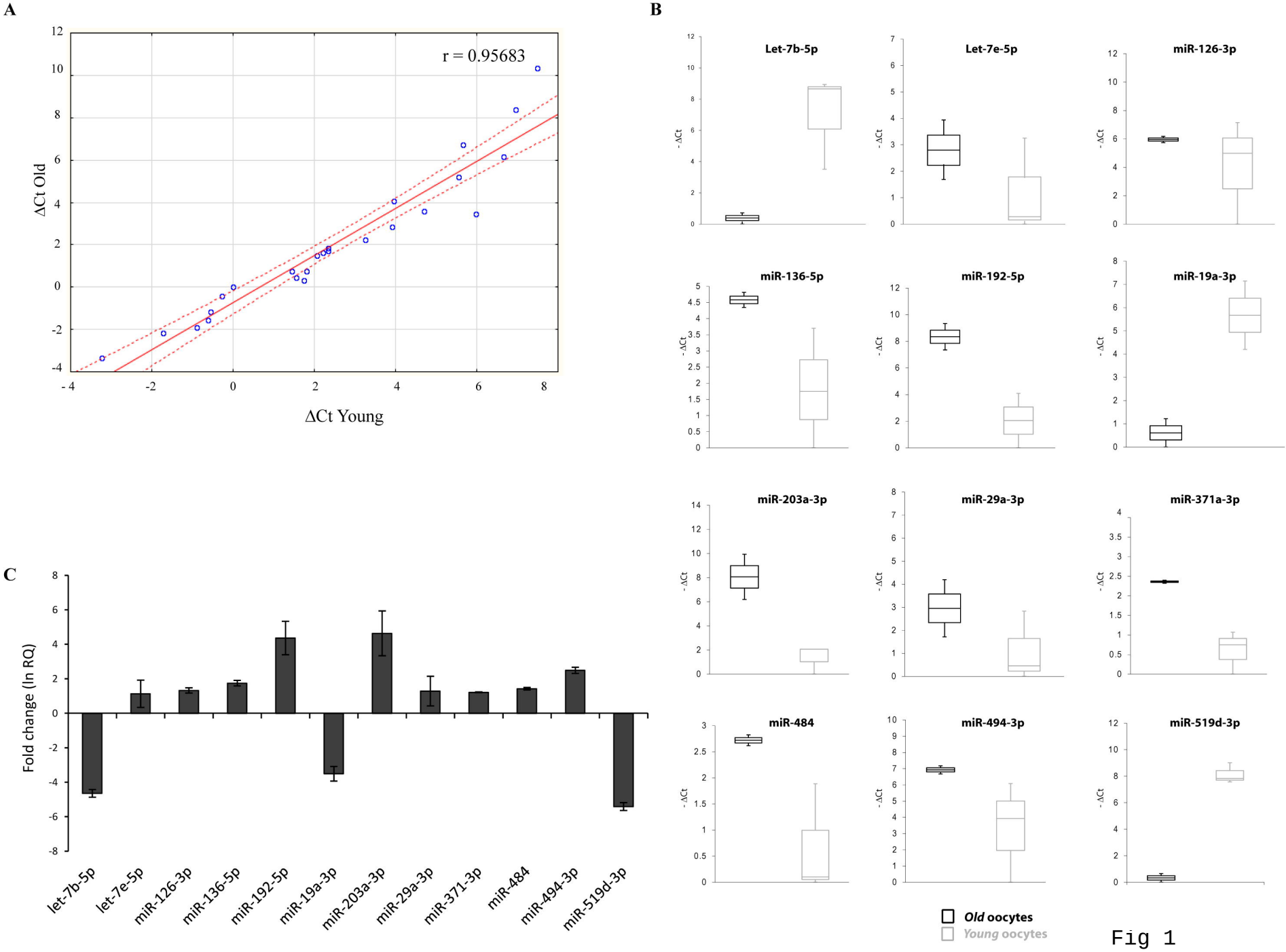
A
r = 0.95683
ΔCt Old
ΔCt Young
B
Let-7b-5p
Let-7e-5p
miR-126-3p
miR-136-5p
miR-192-5p
miR-19a-3p
miR-203a-3p
miR-29a-3p
miR-371a-3p
miR-484
miR-494-3p
miR-519d-3p
- ΔCt
Old oocytes
Young oocytes
C
Fold change (ln RQ)
let-7b-5p
let-7e-5p
miR-126-3p
miR-136-5p
miR-192-5p
miR-19a-3p
miR-203a-3p
miR-29a-3p
miR-371-3p
miR-484
miR-494-3p
miR-519d-3p

Fig 1

miR-371 Cluster

Chr 19 q13.42

53,787,673-53,788,774

hsa-miR-371a	**AAGUGC**CGCCAUCUUUUGAGUGU
hsa-miR-372	A**AAGUGC**UGCGACAUUUGAGCGU
hsa-miR-373	G**AAGUGC**UUCGAUUUUGGGGUGU

miR-17-92 Cluster

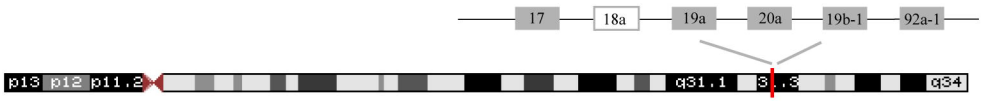

Chr 13 q31.3

91,350,605-91,351,395

hsa-miR-17a	CA**AAGUGC**UUACAGUGCAGGUAG
hsa-miR-19a	U**GUGC**AAAUCUAUGCAAAACUGA
hsa-miR-20a	UA**AAGUGC**UUAUAGUGCAGGUAG
hsa-miR-19b-1	U**GUGC**AAAUCCAUGCAAAACUGA
hsa-miR-92a-1	UAUUGCACUUGUCCCGGCCUGU

miR-106a Cluster

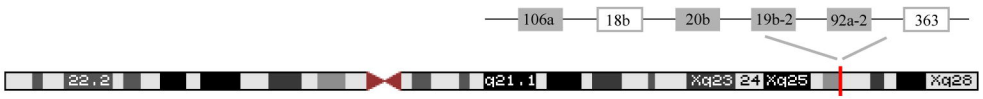

Chr X q26.2

134,169,391-134,170,283

hsa-miR-106a	AA**AAGUGC**UUACAGUGCAGGUAG
hsa-miR-20b	CA**AAGUGC**UCAUAGUGCAGGUAG
hsa-miR-19b-2	U**GUGC**AAAUCCAUGCAAAACUGA
hsa-miR-92a-2	UAUUGCACUUGUCCCGGCCUGU

C19M Cluster

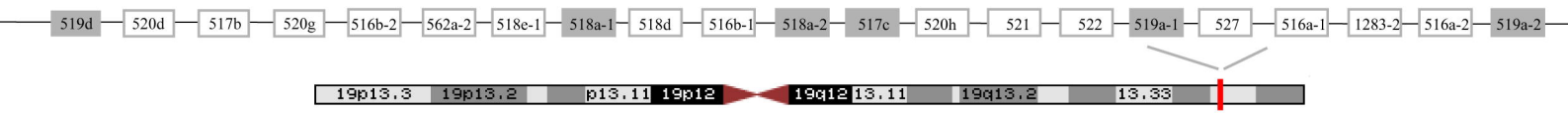

Chr 19 q13.42

53,713,320-53,762,430

hsa-miR-517c	AUC**GUGC**AUCCUUUUAGAGUGU
hsa-miR-518a	GA**AAGCGC**UUCCCUUUGCUGGA
hsa-miR-519a	A**AAGUGC**AUCCUUUUAGAGUGU
hsa-miR-519d	CA**AAGUGC**CUCCCUUUAGAGUG

Fig 2

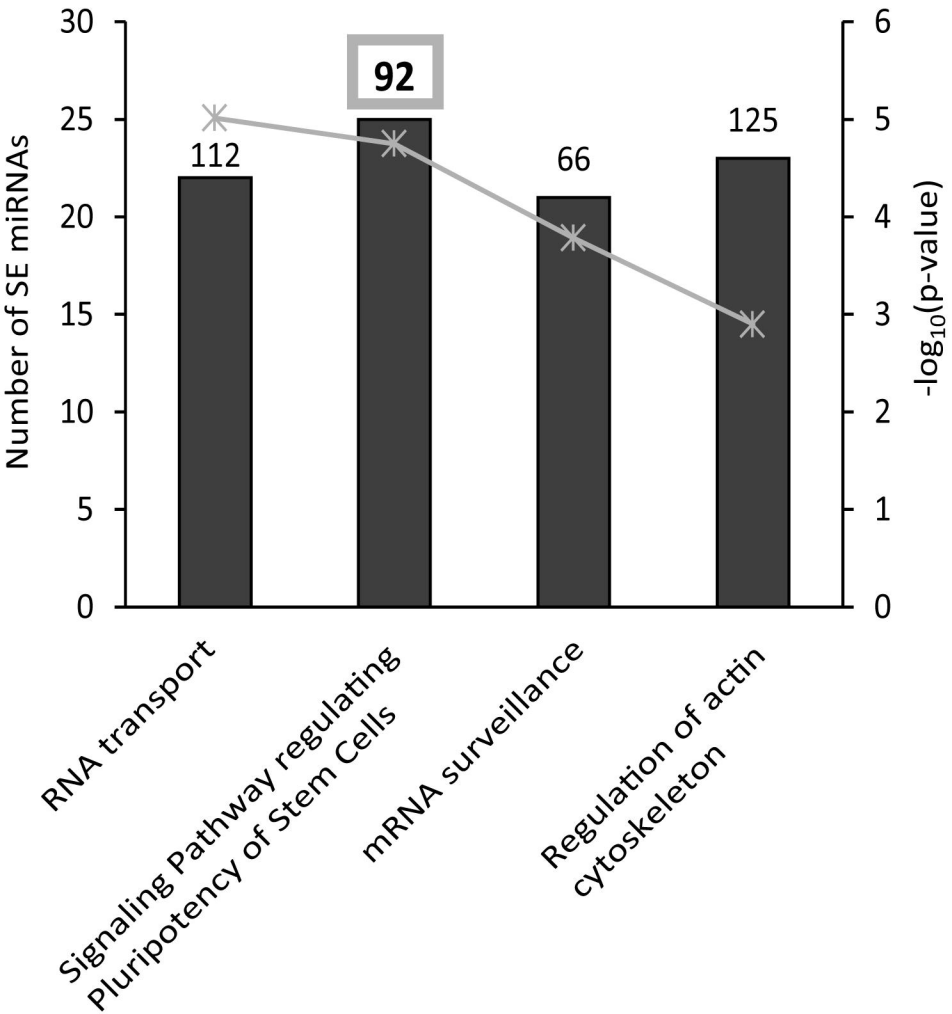

92 GENE TARGETS of SE miRNAs in Signaling Pathways regulating Pluripotency of Stem Cells

BMI1	MAPK14	LIF	WNT3A
PCGF6	TBX3	FZD4	NANOG
JARID2	HAND1	RIF1	PIK3CA
TCF3	FZD6	PIK3R3	IL6ST
GSK3B	RAF1	JAK2	MAP2K1
DVL3	SMAD3	SMAD4	ISL1
STAT3	SMARCAD1	CTNNB1	WNT2
FZD5	INHBA	AXIN2	ID3
OTX1	WNT4	AKT1	FGFR2
ID2	AXIN1	MYC	FGFR1
KAT6A	WNT3	LIFR	MAPK1
PAX6	IGF1R	SKIL	PCGF3
SMAD2	ZFHX3	SMAD5	GRB2
NRAS	ID4	PIK3R1	SMAD1
INHBB	WNT5B	ACVR2A	KLF4
SMAD9	KRAS	MAPK3	LEFTY2
APC	FZD3	FGF2	JAK1
PIK3CB	MAPK13	BMP2	HNF1A
REST	ACVR1	FZD1	WNT9A
ACVR1B	ACVR2B	ACVR1C	BMP4
WNT5A	AKT2	WNT10A	MEIS1
PIK3R2	PCGF5	AKT3	BMPR2
PIK3R5	SETDB1	BMPR1A	PCGF2

Fig 3

A

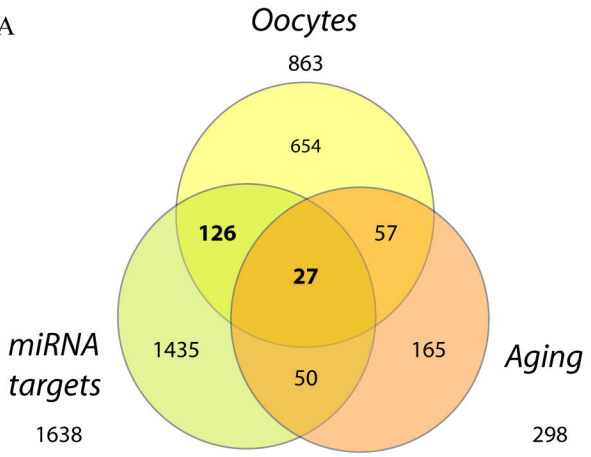

ACACA	HMGA1	PGRMC1
ADM	HOXA5	PIK3R2
ADSS	HPRT1	PRDM2
AGO2	ID2	PRKAA1
ALCAM	IFNB1	PURA
ARHGAP5	IMPDH1	RAB3B
AURKB	IQGAP1	RAN
BIRC5	ITPR1	RAP1A
BLCAP	JAK1	RAP1B
BNIP2	JARID2	RASA1
BRWD1	KIF5B	RBBP7
CDC25A	KLF11	RBFOX2
CDCA8	KLF5	RHOB
CDK2	KLHDC3	RICTOR
CDK6	KPNA2	ROBO1
CENPE	KRAS	RPIA
CHIC1	LANCL1	RRM2
CKS1B	LFNG	SAP30
CLTC	LIF	SCD
CPEB1	LIMK1	SGK1
CPT1A	LONRF1	SHOC2
CTCF	MAD2L1	SLC39A6
CXCR4	MAP2K1	SMARCA1
DCP1A	MAPK1	SMARCA5
DCP2	MAPK6	SMARCAD1
DICER1	MASTL	SMARCD1
DKK1	MBD2	SMC1A
DNMT1	MBD4	SOCS3
DNMT3A	MCL1	SPIRE1
DNMT3B	MCM10	SRC
DUSP19	METAP2	STK38
DUSP7	MSMO1	TFAM
EDN1	NAP1L1	TGFB2
EDNRA	NASP	TGOLN2
EFNB2	NCOA3	TLR4
ESPL1	NCOA6	TMCC1
FOXJ2	NID2	TRIM71
FXR1	NRAS	UBE2A
GAPDH	NUP54	VCAN
GGCT	ORC1	WEE1
GMFB	PDIA3	YWHAE
GSG2	PFKP	ZSWIM3

AKT1
ATM
BLM
CCNA2
CDC42
CDKN1A
CREB1
ERCC3
ERCC6
ESR1
GSK3B
HELLS
HIF1A
HSP90AA1
HSPA8
IL6
LMNA
MAPK14
MXI1
NBN
PIK3CA
PRKCA
PRKDC
SIRT1
TNF
TOP1
PTEN

B

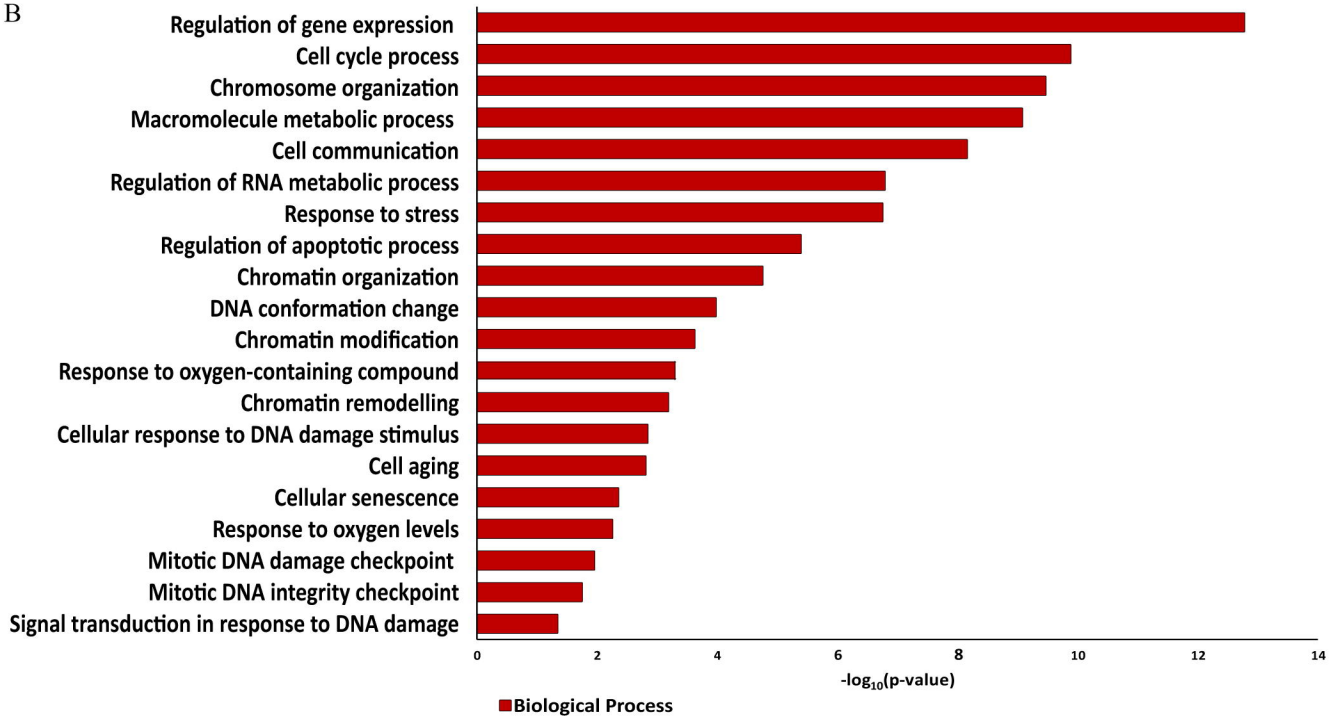

C

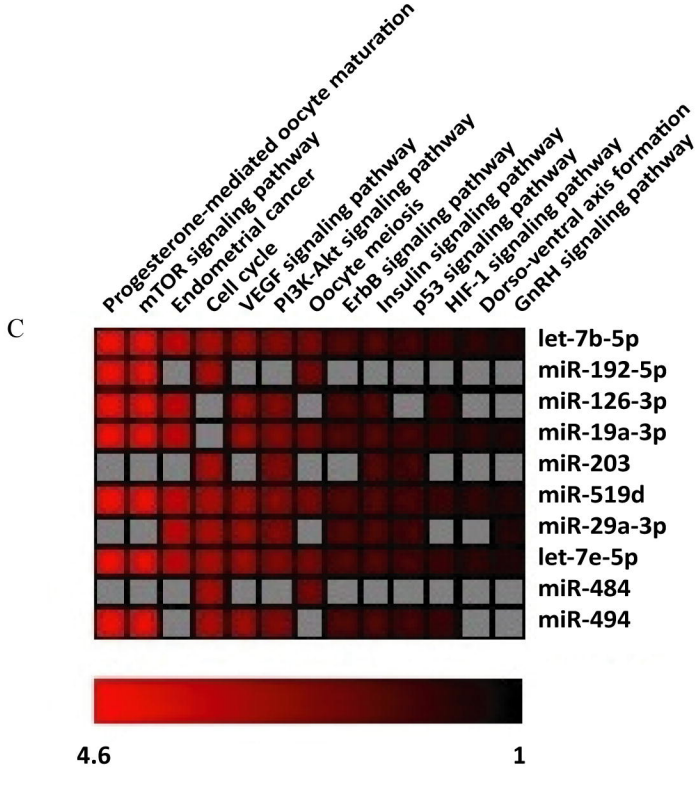

Fig 4

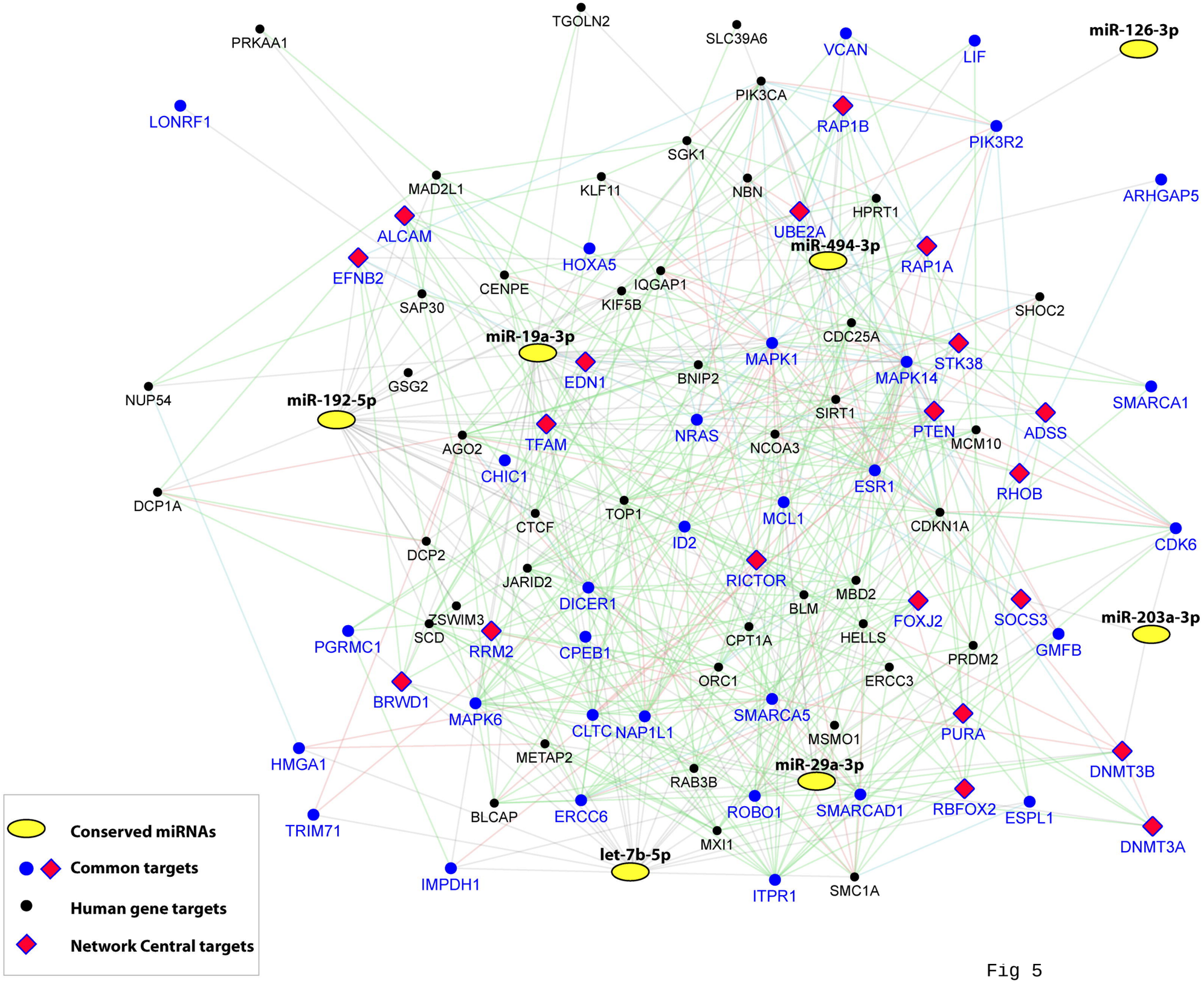
TGOLN2
PRKAA1
SLC39A6
VCAN
LIF
miR-126-3p
PIK3CA
LONRF1
RAP1B
PIK3R2
SGK1
MAD2L1
KLF11
NBN
ARHGAP5
HPRT1
UBE2A
ALCAM
miR-494-3p
HOXA5
RAP1A
EFNB2
CENPE
IQGAP1
KIF5B
SAP30
SHOC2
CDC25A
miR-19a-3p
MAPK1
STK38
EDN1
BNIP2
MAPK14
GSG2
NUP54
SMARCA1
miR-192-5p
SIRT1
PTEN
ADSS
NRAS
TFAM
AGO2
NCOA3
MCM10
CHIC1
ESR1
RHOB
DCP1A
TOP1
MCL1
CTCF
CDKN1A
ID2
CDK6
DCP2
RICTOR
JARID2
MBD2
DICER1
BLM
FOXJ2
SOCS3
miR-203a-3p
ZSWIM3
SCD
CPT1A
HELLS
PGRMC1
RRM2
CPEB1
GMFB
PRDM2
ORC1
ERCC3
BRWD1
SMARCA5
MAPK6
CLTC
NAP1L1
PURA
MSMO1
HMGA1
METAP2
miR-29a-3p
DNMT3B
RAB3B
ROBO1
SMARCAD1
RBFOX2
ESPL1
BLCAP
ERCC6
TRIM71
MXI1
DNMT3A
let-7b-5p
IMPDH1
ITPR1
SMC1A
Conserved miRNAs
Common targets
Human gene targets
Network Central targets

Fig 5

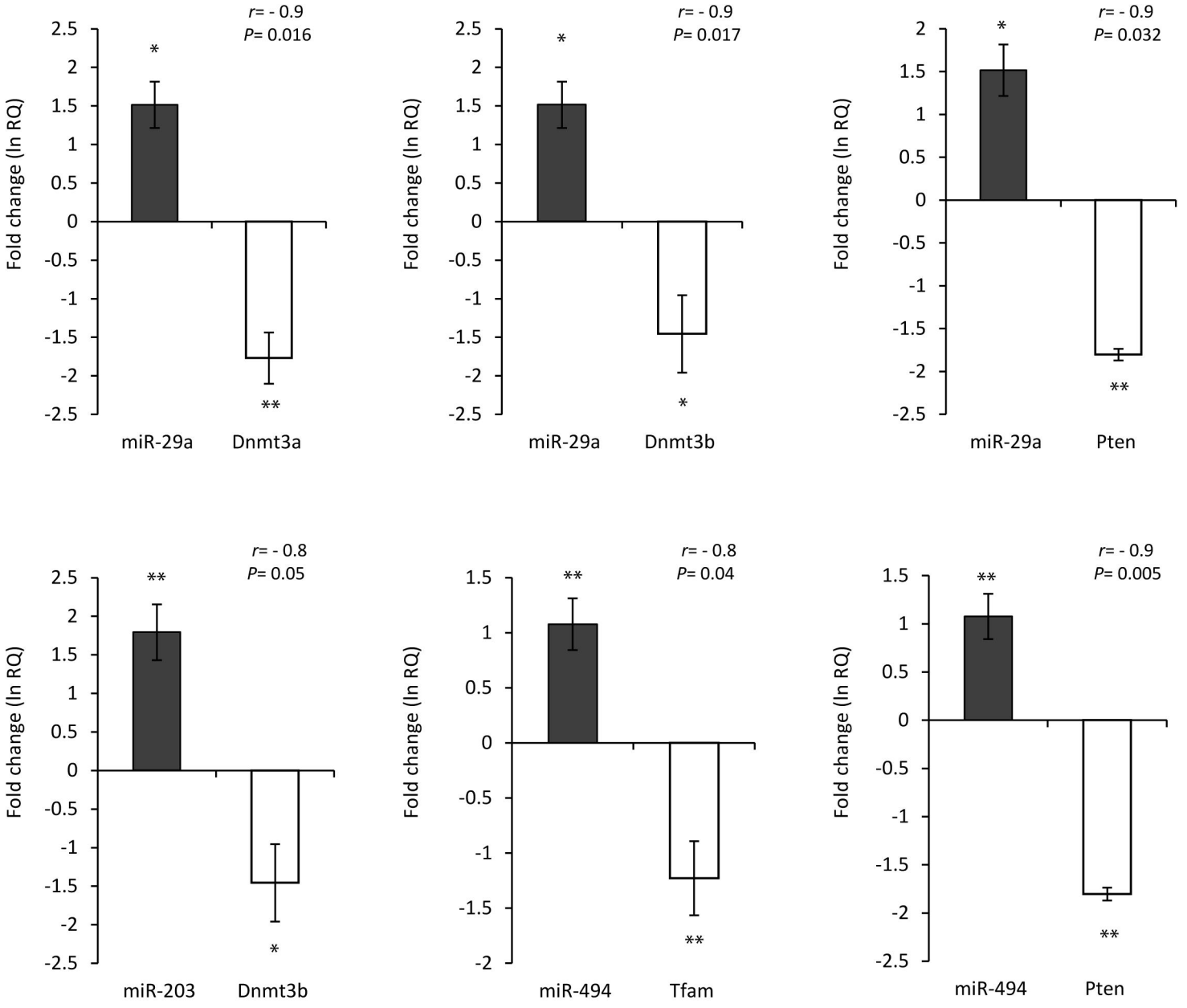
r= - 0.9
P= 0.016
Fold change (ln RQ)
miR-29a
Dnmt3a
r= - 0.9
P= 0.017
miR-29a
Dnmt3b
r= - 0.9
P= 0.032
miR-29a
Pten
r= - 0.8
P= 0.05
miR-203
Dnmt3b
r= - 0.8
P= 0.04
miR-494
Tfam
r= - 0.9
P= 0.005
miR-494
Pten
miRNAs
Target Genes

Fig 6